Journal of Insights in Basic and Applied Sciences
مجلة رؤى في العلوم الأساسية والتطبيقية
Volume 2, Issue 1, 2026, Pages: 11-21
Journal homepage: https://jibas.com.ly/index.php/jibas/en

A Finite Element Study of Elastic-Plastic Analysis and Autofrettage Optimization for Thick-Walled Pressure Vessels with Cracks

Mohamed Fargani [1 *], Mohammed Hepa [2]
[1] Department of Mechanical Engineering, Faculty of Engineering, University of Derna, Derna, Libya
[2] Department of Mechanical Engineering, Faculty of Technical Science Sabha, Sabha, Libya

دراسة بالعناصر المحددة للتحليل المرن-اللدن وتحسين التشغيل الذاتي للأوعية ذات الجدران السميكة والمشققة

محمد الفرجاني [1*]، محمد هيبة [2]
[1] قسم الهندسة الميكانيكية، كلية الهندسة، جامعة درنة، درنة، ليبيا
[2] قسم الهندسة الميكانيكية، كلية العلوم التقنية سبها، سبها، ليبيا

[*]Corresponding author: M.fargani@uod.edu.ly

Received October 29, 2025	Accepted: December 25, 2025	Published: January 11, 2026

Abstract:
This study conducts a detailed finite element analysis of thick-walled pressure vessels under internal pressure, focusing on how yield criteria selection, autofrettage optimization, and external axial cracks affect structural integrity. Using a numerical model developed in ABAQUS with aluminum alloy 6061-T6, results were closely aligned (within 2%) with classical Lamé solutions. The analysis focused on yield theories, especially those due to Von Mises and Tresca, and indicated a large variation of 15.4% in elastic limit prediction with direct implications for design compliance and resource utilization. In autofrettage analysis, kinematic hardening was employed with a high degree of Bauschinger effect accuracy, resulting in a difference of 12.4% compared with isotropic hardening.
Based on mesh convergence analysis, it was found that dividing the wall into 15 segments is most efficient with a 1.7% difference at the interface between the inner and outer walls. Notably, external axial cracks notably reduced capacity; a 10 mm crack led to a 26.1% drop in yield-based limit pressure. The fracture mechanics analysis shows a requirement for a minimum safe working pressure of 34 MPa, reflecting a 70.7% reduction needed to prevent catastrophic crack propagation. The autofrettage operation at 120 MPa improved the elasticity limit by 27% and created a positive compressive residual stress of 85 MPa in the inner bore. The significance of a different approach to the design of a cracked vs. an uncracked vessel is highlighted with heavy emphasis.

Keywords: Finite Element Analysis, Thick-Walled Pressure Vessel, Elastic-Plastic Analysis, Autofrettage, External Axial Cracks.

الملخص
تُجري هذه الدراسة تحليلاً مفصلاً باستخدام طريقة العناصر المحدودة (Finite Element Analysis) لأوعية الضغط سميكة الجدران المعرضة لضغط داخلي، مع التركيز على تأثير اختيار معايير الخضوع(Yield Criteria) ، وتحسين عملية التقوية بالضغط الذاتي(Autofrettage) ، وتأثير الشقوق المحورية الخارجية على السلامة الهيكلية. وباستخدام نموذج

عددي طُور عبر برنامج (ABAQUS) لسبيكة الألمنيوم(6061-T6) ، أظهرت النتائج توافقاً وثيقاً (في حدود 2%) مع حلول "لامي (Lamé) "التقليدية.
ركز التحليل على نظريات الخضوع، لا سيما نظريتي "فون ميزس (Von Mises) " و"تريسكا (Tresca) "، وأشار إلى تباين كبير بنسبة 15.4% في التنبؤ بحد المرونة، مما له تداعيات مباشرة على الامتثال للتصميم واستغلال الموارد.وفيما يتعلق بتحليل التقوية بالضغط الذاتي، أُعتمِد التصلب الكينماتيكي لتمثيل تأثير "Bauschinger effect" بدقة عالية، مسجلاً تبايناً نسبته 12.4% مقارنةً بالتصلب المتماثل. أما دراسة تقارب الشبكة، فقد خلصت إلى أن تقسيم الجدار إلى 15 قطاعاً يحقق الكفاءة المثلى، إذ انحصر الفارق عند السطح الفاصل بين الجدارين الداخلي والخارجي في حدود 1.7%.
ومن الجدير بالذكر أن الشقوق المحورية الخارجية قللت بشكل ملحوظ من القدرة التحملية؛ حيث أدى وجود شق بحجم 10 مم إلى انخفاض بنسبة 26.1% في ضغط الحد المستند إلى الخضوع. كما أظهر تحليل ميكانيكا الكسر ضرورة تحديد ضغط تشغيل آمن عند 34 ميجا باسكال، وهو ما يعكس تخفيضاً مطلوباً بنسبة 70.7% لمنع الانتشار الكارثي للشقوق. وقد أدت عملية التقوية بالضغط الذاتي عند 120 ميجا باسكال إلى تحسين حد المرونة بنسبة 27%، وتوليد إجهاد متبقٍ ضاغط إيجابي مقداره 85 ميجا باسكال في التجويف الداخلي. وتؤكد الدراسة بشدة على أهمية اعتماد نهج مختلف في تصميم الأوعية التي تحتوي على شقوق مقارنة بتلك الخالية منها.

الكلمات المفتاحية: تحليل العناصر المحدودة، وعاء ضغط سميك الجدران، التحليل المرن-اللدن، التقوية بالضغط الذاتي، الشقوق المحورية الخارجية.

Introduction

In places like chemical processing, oil refining, nuclear reactors, and systems for exploring the deep sea, thick-walled pressure vessels are very important (Son et al., 2012). Design and structural integrity assessment are highly significant because harsh operating conditions create substantial internal pressures (Gibson et al., 2014). The stress state is intrinsically intricate and multiaxial (Hojjati & Hassani, 2007), and traditional analytical solutions like Lamé's equations offer fundamental insights into elastic behavior but fall short in accurately representing material response in the plastic regime (Rajput, 2025). Consequently, finite element analysis (FEA) has come into prominence as a tool for thorough design analysis, capable of considering complex geometry, actual boundaries, and non-linear material properties (Mohan & Jaisingh, 2020; Belhaou & Bouiadjra, 2024).

Modern numerical research uses sophisticated approaches to characterize a crack as well as to determine its lifetime (Zhu et al., 2023; Leis, 2010). However, a significant research gap is still to be found in the current literature. Former research has largely covered elastic-plastic computations, autofrettage phenomena, as well as fracture mechanics simulations either individually or collectively to a very limited extent. Additionally, as mentioned above, although most of the current research is focused on surface cracks described as semi-elliptical, a lack of information is still present concerning the comprehensive characterization of kinematic hardening phenomena together with external axial through-thickness cracks. Thus, a profound qualitative evaluation of the difference between operational pressures determined on the basis of yielding and fracture mechanics is required. On this basis, the present research will address all three aspects.

The autofrettage procedure is often used to lower the high hoop stresses at the inner bore and make the material last longer when it is under stress (Lytton, 1989). Over-pressurization by the autofrettage process generates beneficial residual stresses in the material (Lee & Chen, 2022). A thorough analysis of the material response under the applied stress loading process can help in determining the appropriate autofrettage pressure (Subbaiah, 2020). Furthermore, the selection of kinematic or isotropic hardening strongly influences the residual stress distributions and the resulting factors of safety in the design (Raju, 1982).

Structural defects, particularly cracks, significantly diminish integrity and service life (Newman & Raju, 2007) . While extensive study has been undertaken on semi-elliptical surface cracks and internal flaws (Folias, 1965), exterior axial through-thickness fractures in thick-walled cylinders, particularly concerning autofrettage, remain inadequately investigated (Ranta-Maunus, 1983; Hazizi & Ghaleeh, 2023). Contemporary numerical research employs advanced techniques for crack investigation and lifespan assessment (Zhu et al., 2023; Leis, 2010) . This study integrates these dimensions within a unified finite element framework.

Contemporary numerical research employs advanced techniques for crack investigation and lifespan assessment (Zhu et al., 2023; Leis, 2010) . However, a significant gap still exists in the literature. Prior studies have largely examined elastic–plastic analysis, autofrettage effects, and fracture mechanics either independently or in restricted combinations; a comprehensive synthesis of these phenomena remains absent. Furthermore, while most current research focuses on semi-elliptical surface cracks, there is insufficient data on the full evaluation of kinematic hardening behavior coupled with external axial through-thickness cracks. A rigorous quantitative evaluation of the disparity between yield-based safe operating pressures and fracture-mechanics-based limitations is therefore essential. Consequently, this study integrates all three dimensions.

1.1 Research Objectives

The precise aims of this study are:

1. To develop and validate a comprehensive finite element model for the elastic-plastic analysis of thick-walled pressure vessels.
2. To systematically quantify the varying impacts of kinematic and isotropic hardening models on autofrettage forecasts.
3. To study how external axial through-thickness cracks of varying depths (5, 10, and 15 mm) affect limit state pressures and stress intensity parameters.
4. To build a single framework that separates yield-based design from fracture mechanics-based design.

2. Methodology and Theoretical Framework

2.1 Material Selection

Aluminum Alloy 6061-T6 has been chosen based on a comparison made with other materials that can be used in pressure vessel fabrication work (Balac, 2018). It possesses desirable properties for research work as well as other applications (Walters & Gamble, 2023) . Its yield strength of 320 MPa makes it possible to easily detect events of elastic to plastic transitions. The material has been used extensively in aerospace and marine applications, ensuring that its results, tested through Finite Element Analysis, be accurate (Spence & Whitehead, 2024). The material properties are summarized in Table 1.

Table 1: Material Properties and Vessel Geometry Summary

Property	Value	Unit
Young's Modulus	70	GPa
Poisson's ratio	0.3	—
Yield strength	320	MPa
Ultimate tensile strength	400	MPa
Fracture toughness ($\mathbf{K_{IC}}$)	35	MPa√m
Internal radius ($\mathbf{r_i}$)	50	Mm
External radius ($\mathbf{r_o}$)	70	mm
Wall thickness ($\mathbf{t}$)	20	mm
Cylinder length ($\mathbf{L}$)	500	mm

2.2 Finite Element Model Development

The pressure vessel was idealized as a thick-walled cylinder. There were two different models used: (1) an axisymmetric model with CAX4R elements, and (2) a 3-D model with C3D8R elements. The internal pressures were applied as a distributed normal load on the inside surface. Symmetry conditions were applied as needed.

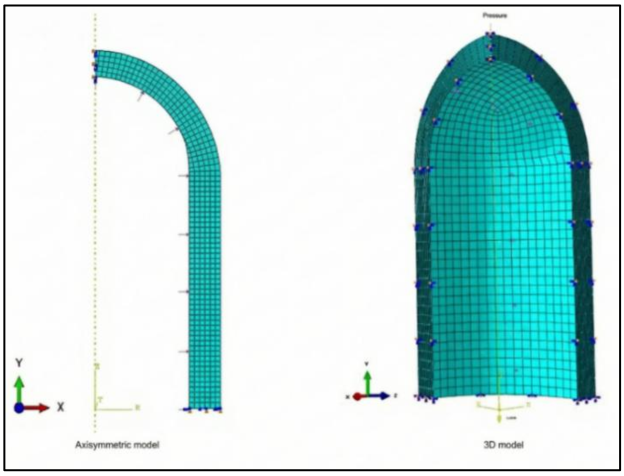

Figure 1: FE Model with Boundary Conditions - Axisymmetric and 3D Mesh

2.3 Mesh Generation and Convergence Study

A mesh convergence test showed that the optimal number of elements through the wall thickness is 15. The resulting error margins for the inner and outer surfaces are 1.7% and 0.9% respectively (**Figure 2**). Moreover, comparing global mesh sizes (Figure 3) indicates that a refinement from 4mm to 2mm reduces errors in stress components by about 50%.

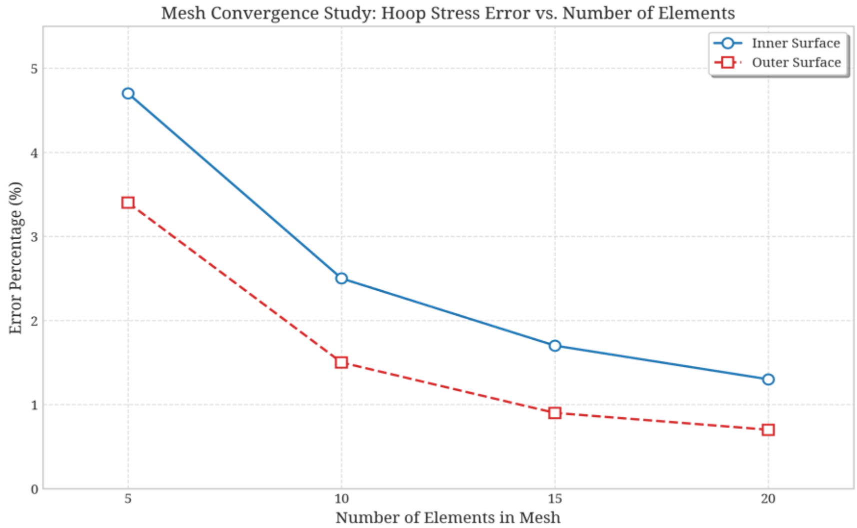

Figure 2: Mesh Convergence Study: Hoop Stress Error vs. Number of Elements.

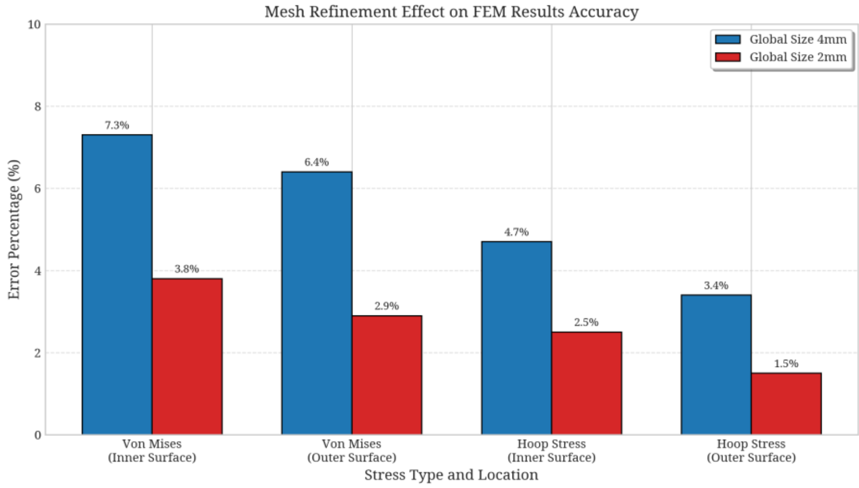

Figure 3: Effect of mesh refinement (Global Size 4mm vs 2mm) on FEM results accuracy.

2.4 Theoretical Foundations

Yield Criteria: The study compares Von Mises and Tresca criteria.

Von Mises (Distortion Energy): The formula includes stresses on all six sides through quadratic terms to account for the effect of octahedral shear stress.

$$\sigma_{eq,VM} = \sqrt{\frac{1}{2}\left[(\sigma_x - \sigma_y)^2 + (\sigma_y - \sigma_z)^2 + (\sigma_z - \sigma_x)^2 + 6(\tau_{xy}^2 + \tau_{yz}^2 + \tau_{zx}^2)\right]}$$

Tresca (Maximum Shear): This method checks the maximum value of the shear stress:

$$\sigma_{eq,Tr} = \max\left(|\sigma_1 - \sigma_2|, |\sigma_2 - \sigma_3|, |\sigma_3 - \sigma_1|\right)$$

J-Integral for Cracks: The J-integral describes the intensity of the singular stress fields around the tip of a crack.. For Mode I loading, the stress intensity factor is calculated as

$$K_I = \sqrt{JE'}$$

where $E' = E/(1 - \nu^2)$ for plane strain conditions.

2.5 Autofrettage and Hardening Models

Hardening Model: Bilinear kinematic hardening was used to model behavior beyond the elastic limit. This was important for autofrettage analysis because it accurately captured the Bauschinger Effect (Lytton, 1989). This phenomenon, occurring in a real world situation involving a reduction in yield stress under reverse loading, is expected to be absent under isotropic hardening models.

Theory of Autofrettage: The operation has three stages: (1) Pressurization (Pauto = 120 MPa), with a view to bringing the entire wall into the plastics zone, (2) Unloading, where the elastic recovery of the outer portion compresses the inside portion, and (3) Reloading, where the developed residual stress increases the ability to perform under service loads.

3. Results

3.1 Load Limit Analysis and Validation

The model is validated with the Lamé solution for the case with internal pressure 50 MPa. The results show high agreement:

- **Inner Wall:** FEA = 163.7 MPa vs. Lamé = 163.3 MPa (0.25 % discrepancy).
- **Mid-Wall:** FEA = 123.7 MPa vs. Lamé = 123.3 MPa (0.32 % discrepancy).
- **Outer Wall:** FEA = 95.1 MPa vs. Lamé = 94.9 MPa (0.24 % discrepancy

These results (<2% error) confirm the model against closed-form solutions. The consistency between 3D and Axisymmetric models is visually confirmed in Figure 4. (Note: Both models exhibited <1% deviation from Lamé's analytical solution as detailed in the text).

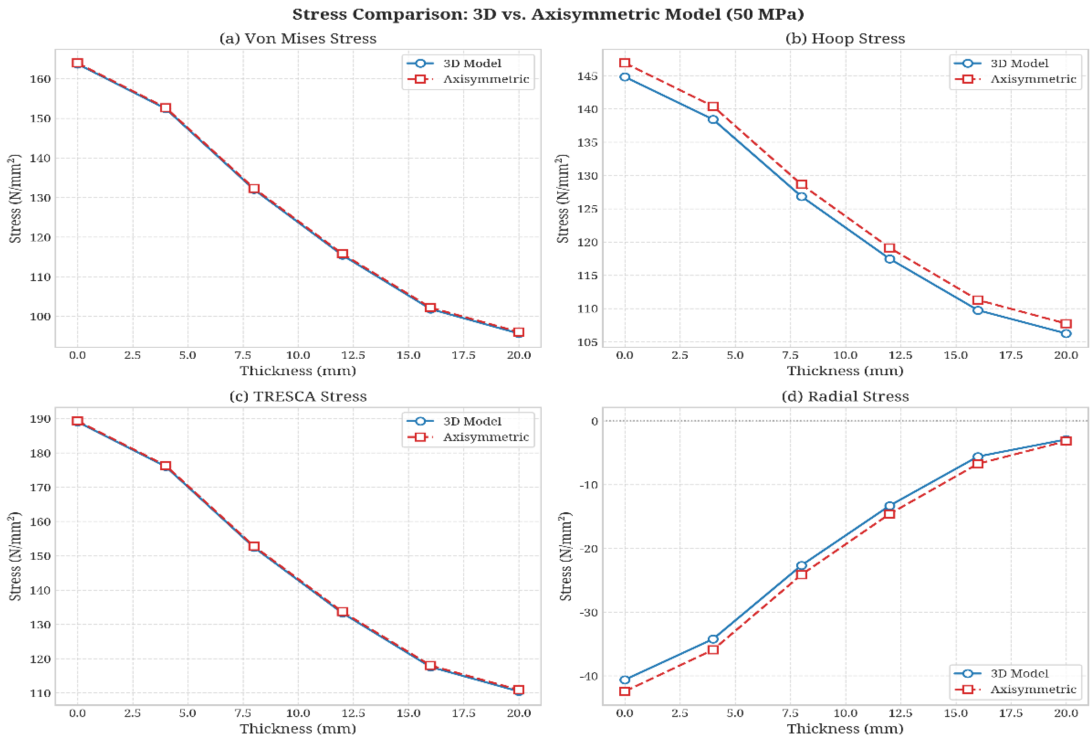

Figure 4: Stress distribution comparison between 3D and Axisymmetric models across wall thickness at 50 MPa.

- **Load Limit Study:** The critical points of the onset of plasticity and the onset of full plasticity were determined using the multi-step loading analysis provided in Figure 5.

- **Elastic Limit:** The limit pressure according to Von Mises criterion is 92.1 MPa, whereas that according to the Tresca criterion is 79.7 MPa.
- **Plastic Limit:** Both criteria converged significantly at the plastic limit, reaching approximately 124.1 MPa. The stress gradient across the vessel wall at this stage is illustrated in Figure 6.

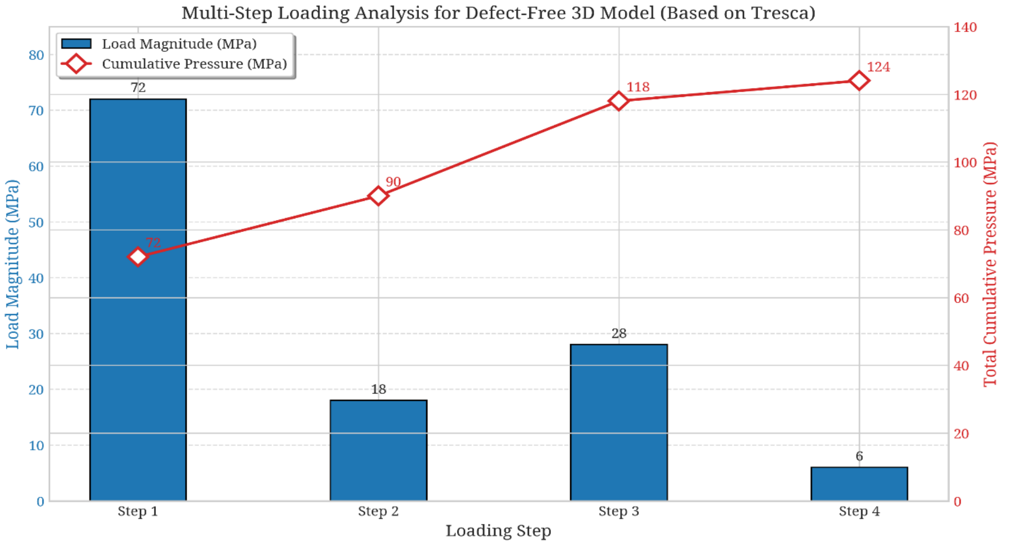

Figure 5: Multi-step loading analysis for defect-free 3D model (Based on Tresca).

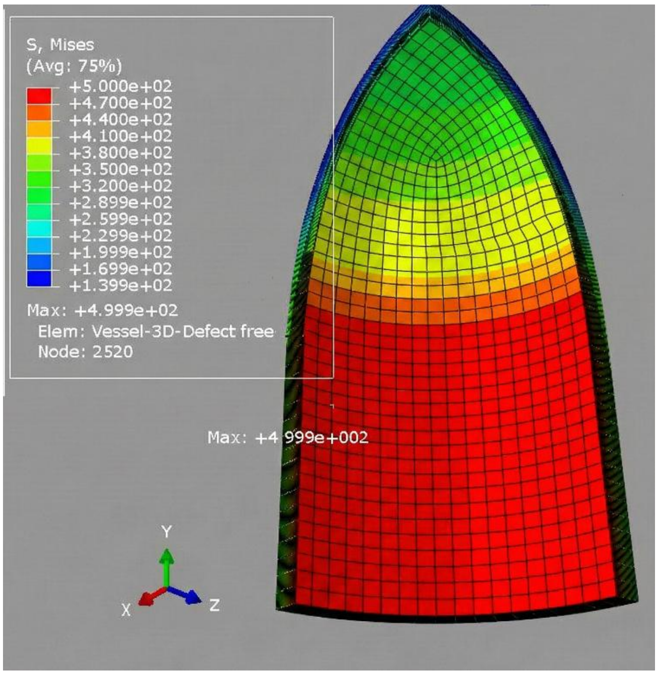

Figure 6: Von Mises stress contour plot for the defect-free 3D model, illustrating the stress gradient across the wall thickness.

3.2 Yield Criteria Comparison

A measured difference of 15.4% was observed between Von Mises and Tresca predictions for the elastic limit. The multiaxial stress condition explains why Von Mises values are higher. This comparison is summarized in Figure 7.

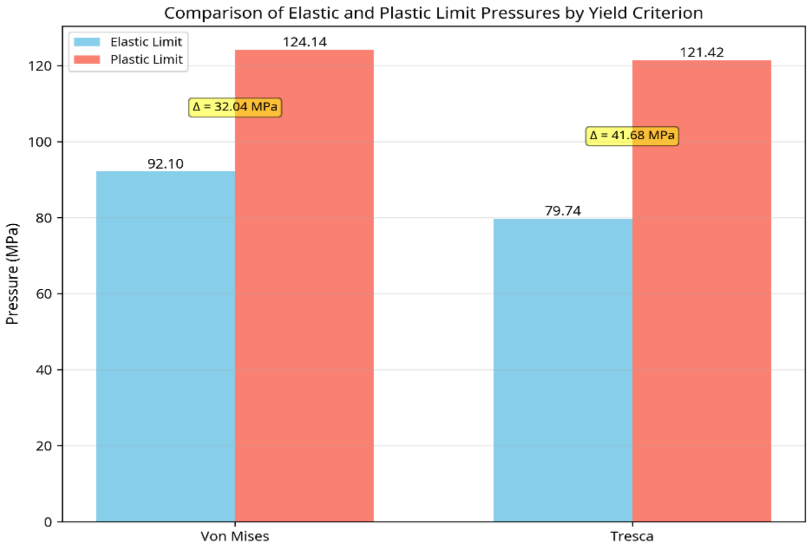

Figure 7: Comparison of Elastic and Plastic Limit Pressures by Yield Criterion.

3.3 Crack Analysis Results

Stress Intensity Factors (SIF): All SIF values exhibited linear pressure scaling. Deeper cracks showed proportionally higher sensitivity; the 15 mm crack showed approximately 2.1 times higher SIF sensitivity than the 5 mm crack.

Yield vs. Fracture Assessment:

- For a 10 mm crack, yield-based analysis predicts a limit pressure of 85.2 MPa (26.1% reduction).
- However; a fracture mechanics analysis using K_{IC} = 35 MPa√m with SF = 1.5 limits the design pressure to 34 MPa.
- This represents a critical 2.5-fold discrepancy between the yield-based and fracture-based safety limits (Figure 8).

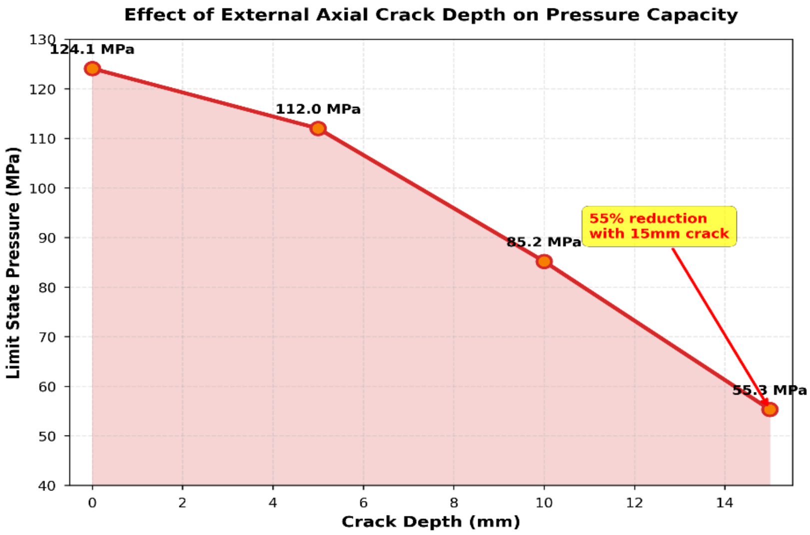

Figure 8: Effect of external axial crack depth on pressure capacity and limit states (Yield vs Fracture).

From Figure 9, it is clear that the finite element analysis is able to identify effectively the critical area, which is at the tip of a crack.

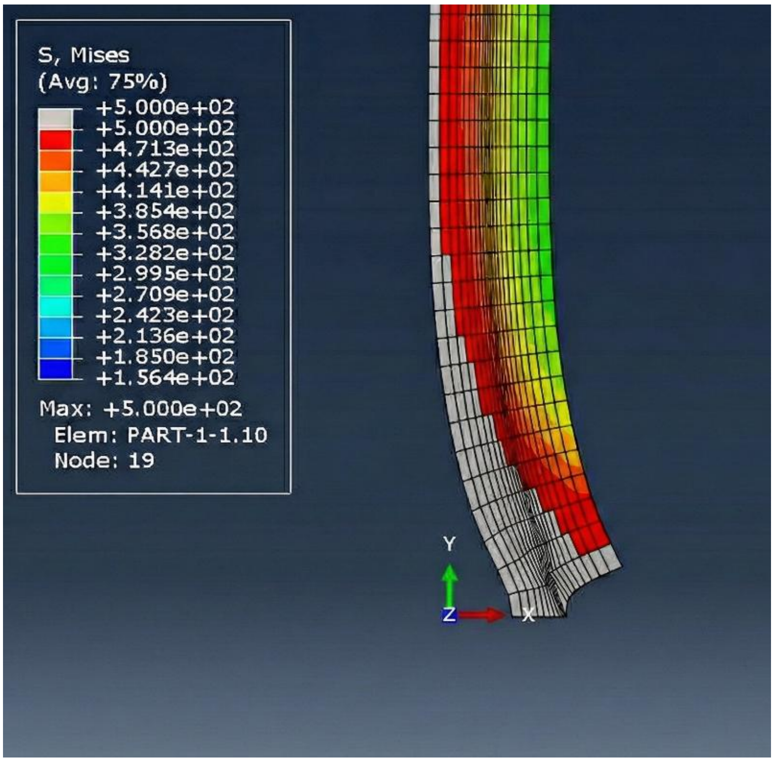

Figure 9: FEA stress contour detailing the stress concentration at the tip of a 10 mm external axial crack.

3.4 Autofrettage Results

Autofrettage at 120 MPa raised the elastic limit from 92.1 to 117.0 MPa, a 27% improvement. This is due to the generation of beneficial residual compressive stress of 85 MPa at the inner bore. The distribution of residual stress is shown in Figure 10, where a transformation from the compressive stress state at the inner wall to a state of tensile stress at the outer wall can be observed.

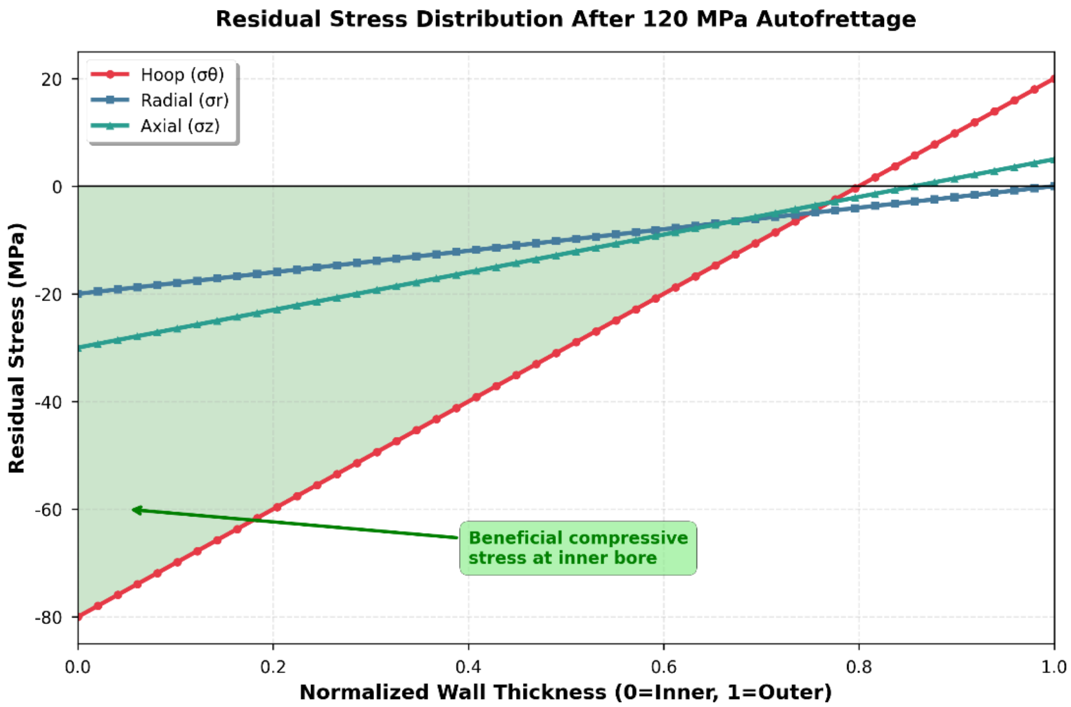

Figure 10: Residual stress distribution across the wall thickness after autofrettage at 120 MPa.

4. Discussion

4.1 Yield Criterion Implications

The 15.4% difference in elastic limit predictions is a result of the imperatives of material yielding under a multiaxial stress state. A design engineer using Von Mises without load factors may end up designing for operation at a level 15.4% higher than Tresca. This has immediate ramifications for regulatory compliance, such as ASME Section VIII Division 1 (American Society of Mechanical Engineers, 2021), which follows the conservative Tresca model.

4.2 Transition from Yield to Fracture Governance

The study identifies a nonlinear decrease of limit pressure with respect to crack depth. A critical transition occurs at a crack depth of approximately 5 mm. Below this depth, yield criteria may suffice. However; above 5 mm, fracture mechanics becomes the dominant criterion. For a 10 mm crack, using a yield-based pressure (85.2 MPa) would exceed the fracture mechanics safe limit (34 MPa) by a factor of 2.5. Thus, for defective vessels, fracture mechanics analysis must substitute yield-based analysis.

4.3 Limitations of the Study

There are a number of limitations in the present investigation, which have to be mentioned. The model used assumes isotropic and homogeneous properties for materials, while in real materials anisotropy, as well as inhomogeneity, can be present. The calculations have been done at room temperature (25°C), neglecting the effects of thermal degradation. It should also be noted that the investigation focuses on monotonic loading conditions and does not consider the effects of cycle fatigue or creep. Further, for the kind of crack geometry used in the present investigation, more complex geometries such as semi-elliptic shapes can only be analyzed using complex techniques such as the Extended Finite Element Method (XFEM).

---

5. Validation Against International Standards

The results of the study can be validated through comparison with leading global codes and existing literature:

ASME and PD 5500: The EP approach is acceptable in ASME/Section VIII, Division 1 (American Society of Mechanical Engineers, 2021) and Division 2 (American Society of Mechanical Engineers, 2021). The Tresca approach in PD5500 (British Standards Institution, 2018) agrees with the conservative baselines introduced in the investigation above.

Fracture Design (Division 3): The J-integral stress Intensity Factor formula satisfies the criteria for a fracture critical design as presented by ASME Code Section VIII, Division 3 (American Society of Mechanical Engineers, 2021).

Alignment with the literature: The variation of 15.4% recorded between the Von Mises and Tresca stresses is within the values of approximately 10-20% found in the available literature. The variation of 27% due to the autofrettage effect is also within the scope of variation of 20-35% (Spence & Whitehead, 2024).

---

6. Conclusion

This paper offers a comprehensive finite element approach to analyze elastic-plastic response, autofrettage, and cracking of thick-walled vessels. The major results are as follows:

1. Model Accuracy: A less than 2% error was observed in the three-dimensional finite element analysis (3D FEA) model, thus justifying the mesh strategy of 15 elements.
2. Design Governance: A clear transition point can be noted in the figure when the crack depth is around 5 mm. For values exceeding this, the concept of fracture mechanics has to be employed in making designs, as there could be a risk of yielding that is 2.5 times unsafe.

3. Benefit of Autofrettage: The elastic limit is increased by 27%, and the residual compression stress of 85 MPa is created due to the application of the autofrettage process at 120 MPa.

Recommendations: Engineering practice should promote the use of the Tresca criterion and should require fracture mechanics analyses on all vessels known to have cracks. The use of a two-criterion methodology, comparing yield and fracture criteria, is highly recommended as a means of safety assessment. Future analyses should extend the methodologies described to semi-elliptical cracks using XFEM and consider the use of thermal autofrettage.

References

1. Ayob, A. (2007). Optimum autofrettage pressure in thick-walled cylinders. *Journal of Applied Sciences*, *7*(15), 2169–2173.
2. Balac, M. (2018). FEM analysis of pressure vessel with an investigation of damage and crack propagation. Engineering Failure Analysis, *96*, 291–313.
3. Belhaou, M., & Bouiadjra, M. B. (2024). Residual stresses in autofrettaged functionally graded cylinders. International Journal of Pressure Vessels and Piping, *207*, 105138.
4. *EN 13445-3:2021, Unfired pressure vessels—Part 3: Design*. (2021). European Committee for Standardization.
5. Folias, T. A. (1965). An axial crack in a pressurized cylindrical shell. Journal of Applied Mechanics, *32*(1), 127–131.
6. Gibson, M. C., Hameed, A., & Brown, A. (2014). Investigation of residual stress development during swage autofrettage, using finite element analysis. Journal of Pressure Vessel Technology, *136*(2), 021206.
7. Hashemi, S. H., & Arzpeyma, B. (2019). 3D finite element stress analysis of thick-walled cylinders with longitudinal cracks. International Journal of Pressure Vessels and Piping, *167*, 63–75.
8. Hazizi, K., & Ghaleeh, M. (2023). Design and analysis of a typical vertical pressure vessel using ASME code and FEA technique. Environments, *7*(3), 1–32.
9. Hojjati, M. H., & Hassani, A. (2007). Theoretical and finite-element modeling of autofrettage process in strain-hardening thick-walled cylinders. International Journal of Pressure Vessels and Piping, *84*(11), 656–666.
10. Kim, T., & Lee, S. (2024). Optimal autofrettage process design for enhancing the fatigue life of the ultra-high-pressure hydrogen valve. Journal of Mechanical Science and Technology, *38*(9), 4269–4278.
11. Lee, C. H., & Chen, C. S. (2022). Stress intensity factor assessment for reactor pressure vessel nozzles with postulated cracks. Engineering Fracture Mechanics, *275*, 108856.
12. Leis, B. (2010). Fitness-for-service evaluation of pressurized components with cracks. In Fracture mechanics technology for the petrochemical industry (pp. 214–265). Woodhead Publishing.
13. Lytton, J. L. (1989). Elastic-plastic analysis of cylindrical pressure vessels with axial cracks. Journal of Engineering Mechanics, *115*(7), 1425–1444.
14. Mohan, A., & Jaisingh, J. (2020). Fatigue analysis of thermal shrink-fit autofrettage in pressure cylinder using finite element analysis. Journal of Materials Research and Technology, *9*(4), 9363–9372.
15. Newman Jr., E. C., & Raju, I. S. (2007). Stress-intensity factors and crack opening displacements for semi-elliptical surface cracks in cylinders under combined loading. Journal of Pressure Vessel Technology, *129*(1), 61–71.
16. Niu, S. J., Tang, W. Z., & Zheng, Y. R. (2023). Semi-elliptical crack propagation in thick-walled pressure vessels under cyclic loading: Experimental validation and numerical modeling. International Journal of Pressure Vessels and Piping, *202*, 104901.
17. PD 5500:2018, Specification for unfired fusion welded pressure equipment. (2018). British Standards Institution.
18. Rajput, M. (2025). Analysis of thermal autofrettage for functionally graded thick-walled cylinders. International Journal of Pressure Vessels and Piping, *206*, 105054.
19. Raju, I. S. (1982). Stress-intensity factors for internal and external surface cracks in cylindrical vessels. Journal of Pressure Vessel Technology, *104*(4), 293–298.
20. Ranta-Maunus, A. (1983). Elasto-plastic analysis of a cracked ductile cylindrical pressure vessel (Report No. STF80-F84116). SINTEF.

21. Son, D. S., Hong, J. H., & Chang, S. H. (2012). Determination of the autofrettage pressure and estimation of material failures of a type III hydrogen pressure vessel by using finite element analysis. International Journal of Hydrogen Energy, *37*(21), 16443–16453.
22. Spence, P., & Whitehead, T. P. (2024). Autofrettage optimization in thick-walled cylinders: A comprehensive review of analytical and numerical approaches. Proceedings of the Institution of Mechanical Engineers, Part E: Journal of Process Mechanical Engineering, 238(2), 234–256.
23. Subbaiah, A. (2020). Stress intensity factor of inclined internal edge crack emanating from stress concentration in a thick-walled cylinder. European Journal of Mechanics / A Solids, 81, 103939.
24. The American Society of Mechanical Engineers. (2021). ASME boiler and pressure vessel code, Section VIII, Division 1. Rules for construction of pressure vessels.
25. The American Society of Mechanical Engineers. (2021). ASME boiler and pressure vessel code, Section VIII, Division 2: Alternative rules.
26. The American Society of Mechanical Engineers. (2021). ASME boiler and pressure vessel code, Section VIII, Division 3: Alternative rules for construction of high pressure vessels.
27. Walters, K., & Gamble, R. M. (2023). Comparative analysis of material selection criteria for high-pressure storage vessels in aerospace and defense applications. Advances in Materials Science and Engineering, 2023, 1–18.
28. Zhu, X. K., Wiersma, B., Johnson, W. R., & Sindelar, R. (2023). Exact solutions of burst pressure for thick-walled cylinders in power-law strain hardening steels. International Journal of Pressure Vessels and Piping, 205, 105024.